Magnetic Circular Dichroism Properties of Reaction Center Complexes Isolated from the Zinc-Bacteriochlorophyll *a*-containing Purple Bacterium *Acidiphilium rubrum*†

Mamoru Mimuro,*,‡ Masayuki Kobayashi,§ Keizo Shimada,|| Katsuhisa Uezono,‡ and Tsunenori Nozawa§

Department of Physics, Biology, and Informatics, Faculty of Science, Yamaguchi University, Yamaguchi 753-8512, Japan, Department of Biomolecular Engineering, Graduate School of Engineering, Tohoku University, Sendai 980-8579, Japan, and Department of Biology, Faculty of Science, Tokyo Metropolitan University, Hachioji 192-0397, Japan

Received June 23, 1999; Revised Manuscript Received January 10, 2000

ABSTRACT: Reaction center (RC) complexes isolated from a Zn-bacteriochlorophyll (BChl) *a*-containing purple bacterium, *Acidiphilium rubrum*, were characterized by absorption, circular dichroism, and magnetic circular dichroism (MCD) spectroscopy. The oxidized-minus-reduced difference spectra indicated that, in this RC, the Zn-BChl *a* is the primary electron donor. The molecular structure of the donor was examined by measuring the ratio of the MCD intensity of the Faraday B-term (*B*) to the dipole strength (*D*). In the Q_y region, *B*/*D* for the donor was about half those of bacteriopheophytin *a* and the accessory Zn-BChl *a*, indicating that the primary electron donor is a dimer. The magnitude of bleach of the Q_x band was half that observed in *Rhodobacter sphaeroides*, suggesting the cation is localized on a single Zn-BChl *a*. The absorption intensity of the higher-energy Q_y exciton band was approximately 28% of that of the lower-energy band, and the exciton splitting was approximately 570 cm^{-1}, smaller than that in *Rb. sphaeroides*. These results indicate that, in *A. rubrum*, the primary electron donor is a Zn-BChl *a* dimer but that the interaction between the two molecules is rather weak. On the basis of these results, an adaptive strategy for changes in BChl *a* species is discussed from an evolutionary perspective.

Acidiphilium rubrum is a purple bacterium found in acidic environments, such as mine drainage having a pH of 3.0 (*1*). It contains a unique pigment, bacteriochlorophyll (BChl)[1] *a*, whose central metal is substituted with Zn (*2*) (hereafter Zn-BChl *a*) (*3*). In this bacterium Zn-BChl *a* is dominant (more than 90%), and a small amount of Mg-BChl *a* is present, whereas Mg-BChl *a* was less accumulated in the membrane preparation (*1*) and in a reaction center (RC) preparation (*4*). A light-induced difference spectrum of membrane preparations showed a peak at approximately 840 nm, a significantly shorter wavelength than that of the purple bacterial RC (*1*). On the basis of this observation and the pigment composition of the preparation, the primary electron donor in this RC appears to be Zn-BChl *a* (*4*). In terms of its electrochemical potential and fluorescence yield, Zn-BChl *a* is expected to show very similar properties to those of Mg-BChl *a* (*5*), however, other organisms containing Zn-BChl *a* have yet to be identified. *A. rubrum* is the only organism in which Zn-BChl *a* is known to play a functional role in nature (*6*). The substitution of the central metal is quite likely to induce a modification in the reaction mechanism; that this bacterium grows in aerobic conditions, similar to *Erythrobacter longus* (*7*), also suggests a modification in the photosynthetic apparatus. Thus, extensive characterization of the RC complex is necessary to better understand the nature of the reactions in *A. rubrum*, especially the ways in which it is similar to or different from other purple bacteria.

Magnetic circular dichroism (MCD) is a circular dichroism (CD) under the presence of a magnetic field along the light path (*8*). In the case of chlorophyll (Chl) or bacteriochlorophyll (BChl), the MCD signal derives from a mixing of the two excited states induced by a magnetic field, the so-called Faraday B-term (*8*). We found that the MCD spectrum of Chl and BChl is very sensitive to the higher-order structure of pigment assemblies in antenna and RC complexes (*9*-*12*). When the dipole strength (*D*) and MCD intensity of the Faraday B-term (*B*) are calculated, and their ratio (*B*/*D*) is estimated, the value of the dimer is almost half that of the monomer in bacterial RC, LH 1, and LH 2 (*9*, *10*). This relationship can also be applied to the primary electron donor in the photosystem (PS) II RC complex and to that in the P_{700}-enriched PS I RC complex (*11*). This is a unique index

* Corresponding author: Tel and Fax +81-83-933-5725; E-mail mimuro@sci.yamaguchi-u.ac.jp.

‡ Yamaguchi University.

§ Tohoku University.

|| Tokyo Metropolitan University.

† This work was supported in part by the Ministry of Education, Science, Sports and Culture, Japan, to M.M. (10440240), to T.N. (07455437), and to K.S. (09309008) and by the Center for Interdisciplinary Research, Tohoku University. Thanks are also due to the Asahi Glass Foundation and to Chugoku Electric Foundation for support to M.M.

[1] Abbreviations: BChl, bacteriochlorophyll; BPheo, bacteriopheophytin; CD, circular dichroism; IR, infrared; LH, light harvesting complex; MCD, magnetic circular dichroism; P_{700}, the primary electron donor of the photosystem I in oxygenic photosynthetic organisms; PMS, phenazine methosulfate; PS, photosystem; RC, reaction center; Zn-BChl *a*, bacteriochlorophyll *a* whose central metal is replaced with Zn.

10.1021/bi991444e CCC: $19.00
Published on Web 03/18/2000

that reflects the higher order structure of pigment assemblies and allows us to estimate the structure of the primary electron donor in the RC complex. We applied this method to an RC preparation isolated from *A. rubrum* and observed that the *B*/*D* of the primary electron donor was almost half that of the accessory Zn-BChl *a* and bacteriopheophytin (BPheo) *a*, which strongly suggests that the primary electron donor in this bacterium was the dimer. Changes in the MCD intensity of the Q_x region suggested that a cation is localized on one Zn-BChl *a* molecule of the special pair. Other findings concerning the molecular organization of the special pair are also reported.

MATERIALS AND METHODS

RC complexes were isolated from membrane preparations of *Acidiphilium rubrum* with the detergent lauryldimethylamine *N*-oxide (LDAO) (0.6%), purified as previously described (*4*), and the samples were suspended in a buffer solution (Tris-HCl, 20 mM, pH 8.0). The preparation still contained LH 1 complex of less than 10% on a protein basis. An RC complex of *Rhodobacter sphaeroides* was prepared as previously described (*13*).

CD and MCD spectra were measured with a Jasco J-720W spectropolarimeter equipped with an electromagnet having a field strength of 1.5 T (*9*−*12*, *14*). All measurements were carried out at 4 °C. The concentration of the RC preparation was approximately 3.3 μM, corresponding to absorbance 0.94 at 793 nm. The isolated RC sample was in the reduced form, and the oxidation was carried out by addition of a minimum concentration of potassium ferricyanide (500 μM) to the sample solution. Absorption spectra were measured with a Beckman UD-640. All spectral data were transferred to a microcomputer for further processing (baseline correction, difference spectrum, and Gaussian deconvolution) (*9*, *11*). The Gaussian deconvolution was carried out based on the least-squares method. Values for the *B*/*D* ratio (*B*, MCD intensity of the Faraday B-term, and *D*, dipole strength) were estimated by the following equations (*9*).

$$D = \frac{9.1834}{\nu_0 \int \epsilon(\nu)\, d\nu} \quad (1)$$

$$B = \frac{(3298 \times 10^4)/33.53}{\nu_0 \int \Delta\epsilon_M(\nu)\, d\nu} \quad (2)$$

where the units for *D* and *B* are square Debye and square Debye × β per cm^{-1} (β is 1 Bohr magneton), respectively; and ν_0 is the resonance frequency. The values for *D* and *B* were estimated on individual bands after deconvolution of the spectra. For the calculation of the dipole strength, a molar extinction coefficient of 288 mM^{-1} cm^{-1} was adopted for accessory Zn-BChl *a* (*15*). The absorption spectra after the measurements were compared with those from before the measurements in order to monitor the degree of light-induced oxidation of the primary donor during the CD and MCD measurements.

Since the addition of potassium ferricyanide disturbed the spectra at wavelengths shorter than 450 nm, the spectral data were shown down to 450 nm. The ambiguity of the wavelength of the CD and MCD spectra was usually no greater than 2 nm and was usually 1 nm in the infrared (IR) region.

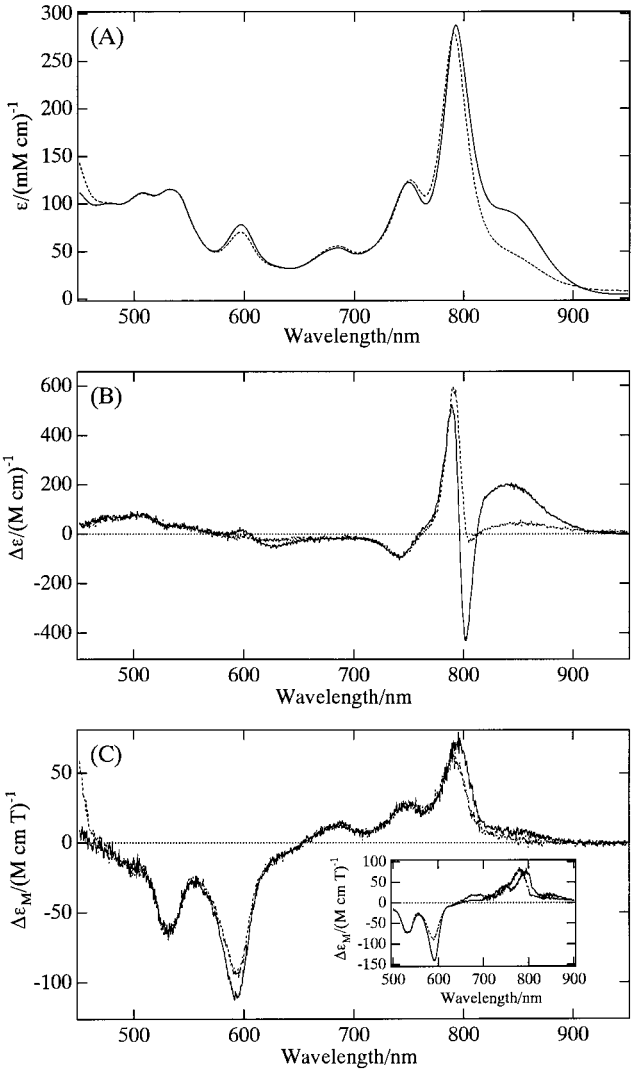

FIGURE 1: Optical properties of RC complex isolated from *A. rubrum* at 4 °C: (A) absorption spectra, (B) CD spectra, and (C) MCD spectra. Solid lines show the spectra of the reduced RC; broken lines show those after oxidation by addition of 500 μM potassium ferricyanide. (Inset) MCD spectrum of a RC preparation of *Rb. sphaeroides*. ϵ, $\Delta\epsilon$, and $\Delta\epsilon_M$ stand for molar extinction coefficient, molar ellipticity, and magnetic molar ellipticity, respectively. The concentration of RC complexes was approximately 3.3 μM.

RESULTS

1. Absorption, CD, and MCD Spectra in the Reduced Form. The isolated RC preparations were in the reduced form, thus the addition of sodium ascorbate (1 mM) and 15 μM phenazine methosulfate (PMS) induced no substantial change in the optical properties (data not shown). In the following experiments, RC preparations were used without the addition of a reductant.

In the IR region, three absorption maxima were detected at 749, 793, and 842 nm (Figure 1A, solid line) corresponding to BPheo *a*, the accessory Zn-BChl *a*, and the primary electron donor (Zn-BChl *a*), respectively. The peak wavelength of BPheo *a* was consistent with that in *Rb. sphaeroides*, and that of the accessory Zn-BChl *a* was about 10 nm shorter than that of the RC complex in *Rb. sphaeroides* (*16*,

17). This is a direct reflection that the absorption maximum of Zn-BChl *a* in organic solvents is located at a shorter wavelength than that of Mg-BChl *a* (*1*). On the other hand, the absorption peak of the primary electron donor was significantly shorter than that of the purple bacterial RC; compared with that in *Rb. sphaeroides*, it was shorter by approximately 30 nm (*16*, *17*). The peak wavelength of the primary donor in *A. rubrum*, however, was identical to that observed by the transient absorption change (*1*). The Q_x band of Zn-BChl *a* was observed at 596.5 nm, while that of BPheo *a*, which was expected at about 540 nm, was not clear due to an overlap with the carotenoid absorption. Absorption bands originating from the carotenoid(s) were discernible at 477.5, 507.5, and 532.5 nm.

The CD and MCD spectra without a reductant were identical to those observed in the presence of 1 mM sodium ascorbate and 15 μM PMS. The CD spectrum corresponded to the absorption spectrum (Figure 1B, solid line); there was a positive signal from the primary electron donor at 843 nm, a large positive signal from the accessory Zn-BChl *a* with a peak at 789 nm, and a small negative band of BPheo *a* at 741.5 nm. The latter was significantly shorter than the absorption band, although the reason for this was not clear. A blue shift of the BPheo *a* peaks in the CD spectra has been reported for other purple bacteria (*18*, *19*). We observed a large negative band with the peak at 803 nm. The CD band corresponding to Q_x bands of BChl *a* was located at 596 nm, whereas that of BPheo *a* was barely observable.

The MCD spectrum of the RC complex showed three peaks in the IR region (Figure 1C, solid line); the locations of the individual maxima were consistent with those in the absorption maxima within $\pm$1 nm, although the intensities of the three bands were different. The MCD intensity of the primary electron donor was quite low; an intensity ratio of the accessory Zn-BChl *a* to the primary electron donor was higher in the MCD spectrum than in the absorption spectrum. This clearly showed that the $\Delta\epsilon_M/\epsilon$ (ϵ, molar extinction coefficient; $\Delta\epsilon_M$, magnetic molar ellipticity) value of the primary electron donor was lower than that of the accessory Zn-BChl *a*. The MCD signals from the Q_x bands of Zn-BChl *a* and BPheo *a* were found at 593 and 531 nm, respectively. Their intensities were higher than those of the Q_y band, which was a typical observation with the MCD spectroscopy of Chl *a* (*20*, *21*) and BChl *a* (*22*) and was consistent with that in the purple bacteria (Figure 1C, inset) (*9*, *10*, *23*).

The absorption spectra after measurement of the CD and MCD spectra were the same as that prior to those measurements, indicating that there was no light-induced oxidation of the primary electron donor. Some variation of the spectra was observed, depending on the preparations, although all variation was confined to the intensities. In the absorption spectra, the ratio A_{793}/A_{840} varied less than 10%, and in the CD spectrum, $\Delta\epsilon_{793}/\Delta\epsilon_{840}$ varied by no more than 20%. The ratio of the CD intensity between the accessory BChl and the primary electron donor is reportedly much greater depending on the preparations and bacterial species (*18*, *19*, *23*−*27*). By contrast, we found that the ratio of the MCD intensities at 750, 792, and 840 nm in preparations of *A. rubrum* was almost constant within the experimental error (data not shown).

2. Absorption, CD, and MCD Spectra in the Oxidized Form. Upon oxidation of the RC preparation with potassium ferricyanide (500 μM), the absorbance of the primary electron donor decreased to about half in the Q_y region, but a significant fraction remained (approximately 50%) (Figure 1A, broken line). Other features included a blue shift of the maximum of the accessory Zn-BChl *a* by 1.5 nm and a red shift of the BPheo *a* by 1 nm. These changes were also observed in the RC complex of *Rb. sphaeroides* (*16*, *17*) and *Chromatium tepidum* (*25*), except for the residual part of the primary electron donor. In the Q_x region, a bleach was detected at 596 nm, although its magnitude was small.

The CD spectrum in the Q_y region changed drastically (Figure 1B, broken line). Oxidation caused the positive CD band of the primary electron donor to nearly disappear, although a small fraction was still observed. Changes in the wavelength region of the accessory Zn-BChl *a* were significant; the negative band at 803 nm almost disappeared and the positive band at 792 nm was enhanced by about 10% and red-shifted to 794 nm. By contrast, there was no substantial change in intensity in the Q_y band of BPheo *a*. Since the disappearance of the large negative CD band at 803 nm was accompanied by the disappearance of the 840-nm band of the primary electron donor, the 803-nm component was assigned to the primary electron donor, which was probably the higher exciton state of the primary electron donor (hereafter the Q_y^+ state; the 842-nm band is hereafter the Q_y^- state). This behavior of the CD spectrum was qualitatively consistent with those observed in *Rb. sphaeroides* (*16*−*19*), *Rhodobacter capsulatus* (*26*), *Rhodospirillum rubrum* (*24*), *Ectothiorhodospira* sp. (*27*), *Rhodospirillum sodomense* (*23*), and *C. tepidum* (*25*). In the Q_x region, we observed the bleach of the band at 596 nm.

The MCD spectrum in the Q_y region also changed along with the changes in the CD spectrum (Figure 1C, broken line). The band intensity of the primary electron donor decreased to less than half, although it still remained. Oxidation of the primary electron donor caused the band of the accessory Zn-BChl *a* to show a blue shift of a few nanometers as observed in the absorption spectrum, and the decrease in the intensity was greater than that of the primary electron donor. There was no significant change in the intensity of the BPheo *a* band. The Q_x band of the primary electron donor was detected at 593 nm and its intensity decreased by 14% from the reduced form. The Q_x band intensity of the BPheo *a* was constant even after oxidation.

The RC preparation used in this study showed partial irreversibility of the spectral changes and its magnitude was approximately 20% that of the original samples. The difference spectra induced by the second treatment were essentially identical to those observed for the first treatment. This indicated that some of the special pairs underwent irreversible inactivation after oxidation by ferricyanide, while the rest did not.

3. Difference Spectra Induced by Oxidation of the Special Pair. The difference (oxidized minus reduced) absorption spectrum (Figure 2A) clearly indicated a bleach of the Q_y^- state at 844 nm, a blue shift of the accessory Zn-BChl *a* with a zero crossing point at about 792 nm, and a red shift of the BPheo *a* with a zero crossing point at about 746 nm. The magnitude of the negative band at 803 nm was larger than that of the counterpart positive band of the accessory Zn-BChl *a*, suggesting that an additional component giving a negative signal was present in the long-wavelength region

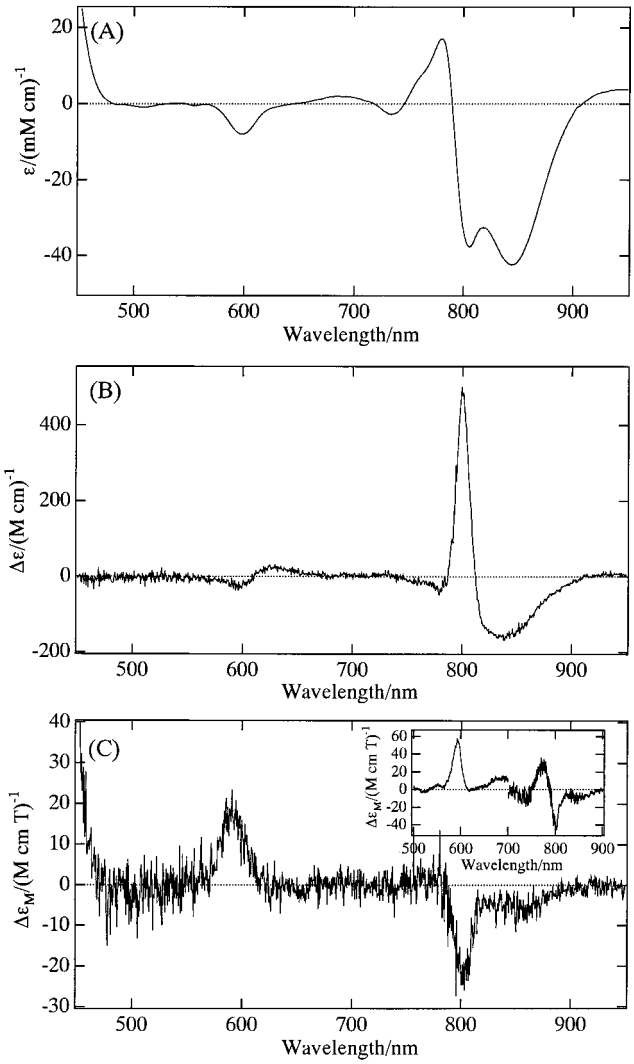

FIGURE 2: Difference spectra induced by oxidation of the primary electron donor in the RC complex of *A. rubrum*: (A) difference absorption spectrum, (B) difference CD spectrum, and (C) difference MCD spectrum. (Inset) Difference MCD spectrum of a RC preparation of *Rb. sphaeroides*. Absorption, CD, and MCD spectra of one sample were measured in the reduced form, and potassium ferricyanide was added to the same sample. The spectra were stored in a microcomputer, and the difference spectra were calculated numerically.

of the 803-nm peak (Q_y^+ state). In the Q_x region of Zn-BChl *a*, a negative peak was observed at 598 nm, corresponding to a bleach of the primary electron donor. In the difference CD spectrum (Figure 2B), two kinds of signals were observed; one was a bleach of the primary electron donor at about 838 nm, and the other was a large positive band at 799.5 nm, corresponding to the Q_y^+ state. A bleach of the Q_x band of the primary electron donor was detected at 597 nm in addition to an increase in the band at 625 nm. The origin of the latter band was not clear, although a comparable band was detected in the RC preparation of *C. tepidum* (*23*, *25*). In the difference MCD spectrum (Figure 2C), some changes in the primary electron donor were observed; there was a bleach of the lower exciton band at 840 nm (Q_y^- state) and the higher exciton band at 800 nm (Q_y^+ state). In the Q_x region, a difference maximum was observed at 591 nm.

As a reference, we measured the MCD spectra of an RC preparation of *Rb. sphaeroides* (Figure 1C, inset). The overall spectrum was very similar to that of *A. rubrum* for the reduced (solid line) and oxidized (broken line) conditions; however, a significant difference was observed in the difference spectrum (Figure 2C, inset). There were three kinds of signals in the Q_y region in *Rb. sphaeroides*: a bleach of the Q_y^- state (870 nm), a bleach of the Q_y^+ state (810 nm), and a shift of the accessory BChl *a* with a zero crossing point at about 795 nm. The magnitude of intensities due to the band shift was larger than the bleach of the Q_y^+ and Q_y^- states. A shift-type difference spectrum was not observed in *A. rubrum*.

We found a remarkable spectral feature of the *A. rubrum* RC complex using the three kinds of difference spectroscopy, namely, a significant signal from the upper exciton level of the primary electron donor at 803 nm, which is not as significant in other purple bacteria (*16*−*19*). This suggests a difference in the molecular arrangement of the primary electron donor from that of the purple bacteria (*16*−*19*, *23*−*29*).

4. Gaussian Deconvolution of the Spectra. Absorption, CD, and MCD spectra were deconvoluted into component bands with a Gaussian shape (Figures 3 and 4). We attempted to set the following initial conditions for simulation: we assumed the minimum number of components and spectral components were common in terms of their wavelengths and bandwidths among the three spectra, and so we set the variables to the amplitudes. We also set the following two conditions: first, a component corresponding to LH 1 was included in the calculation since less than 10% of our RC preparation was still contaminated by LH 1; and second, the difference spectra were simulated to reproduce the bleach of the primary electron donor, a blue shift of the accessory Zn-BChl *a*, and a red shift of the BPheo *a*. The spectral parameters of the membrane preparations were estimated to apply to deconvolution of the RC preparations. We used membranes in the oxidized condition since the contribution of RC in this preparation was minimal (Figure 5). The 862.4-nm absorption band, 871.5-nm CD band, and 862.3-nm MCD band were resolved on the membrane preparations. The 862.4-nm absorption peak of the Zn-BChl *a* was not consistent with the 852-nm peak of the reconstituted sample (*30*). Compared with LH 1 of purple bacteria, a blue shift of about 10 nm was observed, and this difference was consistent with the difference of the peak of Zn-BChl *a* and Mg-BChl *a* in organic solvents (*1*, *31*).

Table 1 summarizes the parameters for the simulation calculations we obtained. The simulation parameters that most precisely reproduced the three kinds of spectra in the reduced and oxidized forms and their respective difference spectra were selected. We resolved the locations of the absorption peaks of the Q_y^- state, the accessory Zn-BChl *a*, and BPheo *a* in the reduced form to 844.6, 792.0, and 749.9 nm, respectively (Figure 3). A blue shift of the accessory Zn-BChl *a* and a red shift of BPheo *a* upon oxidation were reproduced by the deconvolution (790.8 and 751.0 nm, respectively; Table 1, oxidized form, and Figure 4). In the CD spectrum of the reduced form (Figure 3B), the magnitude of the 800.6-nm negative band was larger than the actual band intensity; this was simply due to compensation of the magnitude of the positive band at 792.0 nm. This was also the case for the oxidized form where there was not a substantial negative signal (Figure 4). Since the locations of

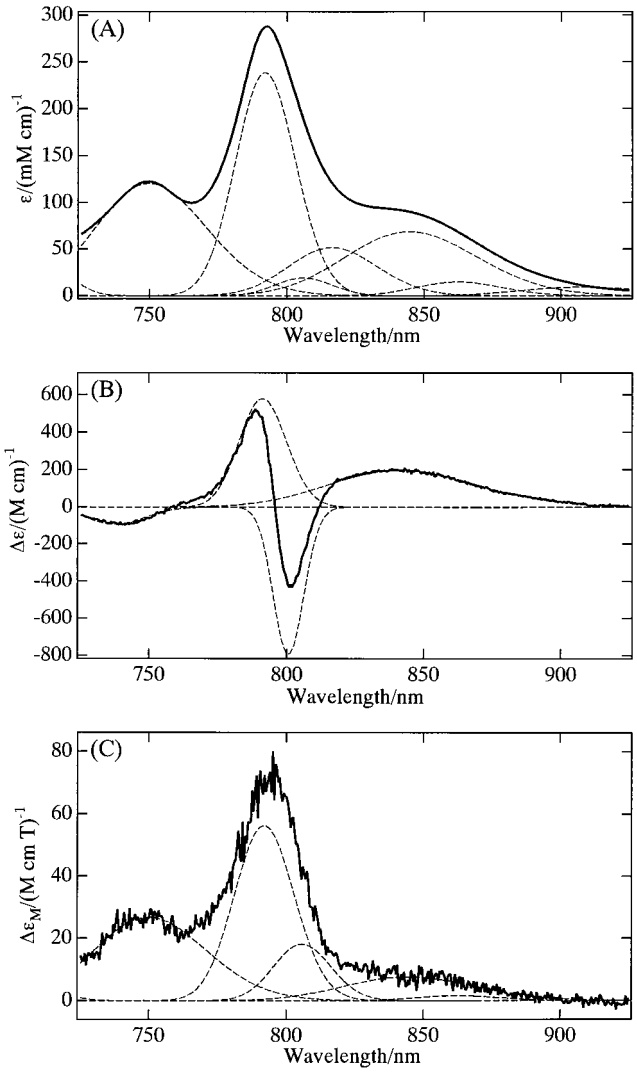

FIGURE 3: Estimation of components by deconvolution of three kinds of spectra in the reduced form: (A) absorption, (B) CD, and (C) MCD spectra of RC complex in the reduced form (Figure 1, solid lines). Simulated curves are shown by broken lines, and parameters for fitting are given in Table 1.

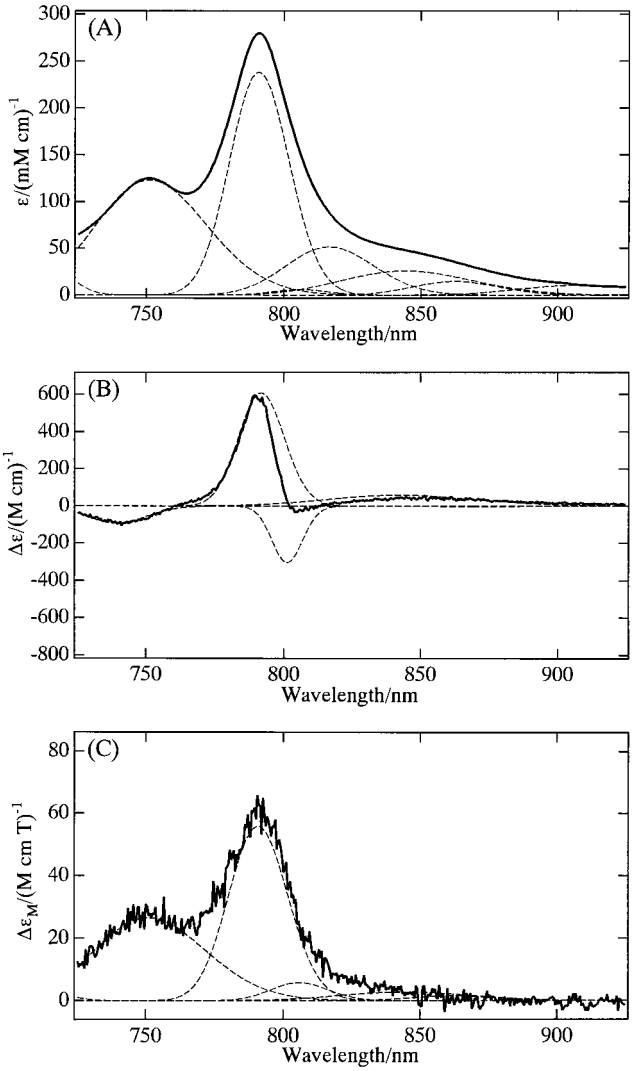

FIGURE 4: Estimation of components by deconvolution of three kinds of spectra of the oxidized RC complex: (A) absorption, (B) CD, and (C) MCD spectra of RC complex in the oxidized form (Figure 1, broken lines). Simulated curves were shown by broken lines, and parameters for fitting were shown in Table 1.

the two CD bands were close to each other, it was appropriate to estimate the magnitudes of the individual bands by deconvolution. While the absorption components corresponded well to the MCD components, the peak locations of the two components in the CD spectra were not consistent with either the absorption or MCD spectra. The 749.9-nm BPheo *a* band was resolved to 737.5 nm, because the observed CD peak of BPheo *a* was located at 742 nm (Figure 1B). The reason for the large blue shift was not clear. Similarly, the 805.8-nm band was resolved to an 800.6-nm negative band in the CD spectrum (Figure 3B), and the reason for this was also unknown. Even with this ambiguity in the locations of the peak in the CD spectrum, three spectra were resolved by common components. Hereafter, we used the parameters shown in Table 1 to estimate the magnitudes of the individual components.

Changes in the intensities due to oxidation were remarkable in the primary electron donor (Q_y^- and Q_y^+ states), i.e., the absorption bands at 844.2 and 805.8 nm, the CD bands at 842.1 and 801.3 nm, and the MCD bands at 844.1 and 805.8 nm (Figure 4). Compared with the intensities of the corresponding band in the reduced form, the band intensities decreased to 38% and 32% for absorption of the Q_y^- and Q_y^+ states, respectively. Similarly, the band intensities decreased to 30% and 38% for the CD spectra and to 36% and 32% for the MCD spectra. On average, 35% of the original intensities remained after oxidation; this was probably due to the presence of an inactive RC. By contrast, the band intensities of the accessory Zn-BChl *a* and BPheo *a* were nearly identical under the two conditions. These deconvolution patterns well reproduced the difference absorption, the difference CD, and the difference MCD spectra (data not shown). For the simulation calculation, we set one absorption band at 816.3 nm. The corresponding CD and MCD components showed very small amplitudes (less than 0.1% of the band intensities of the accessory Zn-BChl *a*) even when we took this component into account; thus they were negligible. These low amplitudes resulted from the fact that the accessory Zn-BChl *a* band with constant intensities and the primary electron donor band with variable intensities were high enough to fit the CD and MCD spectra. This was not the case for the absorption spectra, however. The origin of this component was not yet determined at this stage in the experiment.

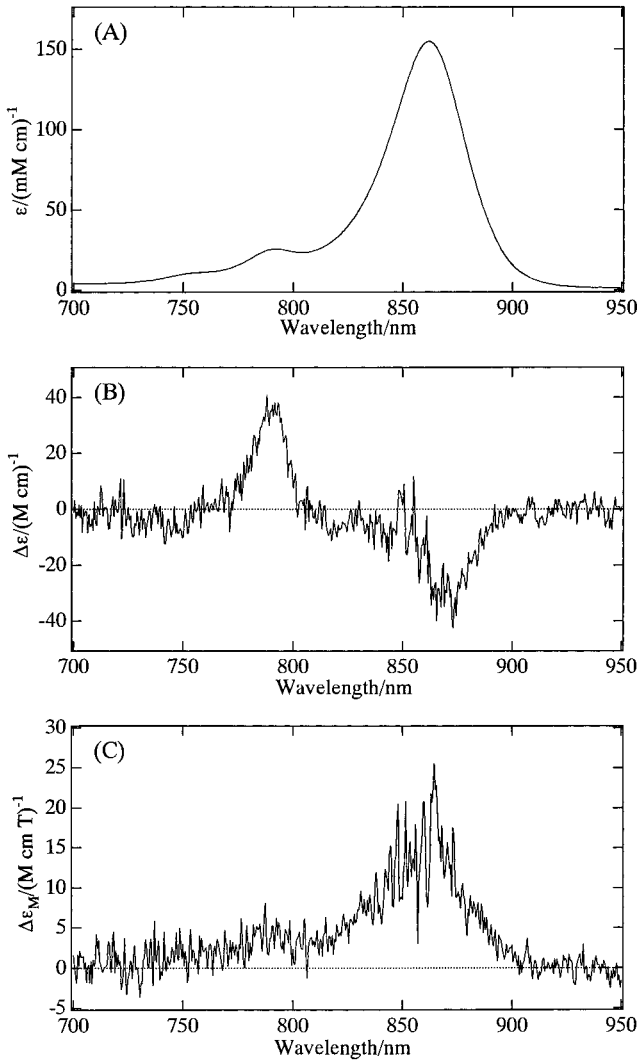

FIGURE 5: Optical properties of membrane preparations of *A. rubrum*: (A) absorption, (B) CD, and (C) MCD spectra in the oxidized forms treated with 500 μM potassium ferricyanide. The membrane preparations were suspended in 20 mM Tris-HCl buffer (pH 8.0).

On the basis of the above deconvolution pattern, we estimated the B/D value for the Q_y^- state of the primary donor, the accessory Zn-BChl *a*, and the BPheo *a* as 11.8, 25.2, and 23.9 for the reduced form and 11.4, 25.0, and 23.1 for the oxidized form, respectively. The *B*/*D* values of components sensitive to oxidation were 11.6, 25.1, and 23.5, respectively, for the Q_y^- state, the accessory Zn-BChl *a*, and BPheo *a*. The values for the Q_y^- state of the primary donor were almost half of those of the accessory Zn-BChl *a* and BPheo *a*. This finding was similar to those found in bacterial RC, LH 1, and LH 2 (*9*, *10*) and PS I RC and PS II RC in the oxygenic photosynthetic organisms (*11*) and thus strongly suggests that the primary electron donor of *A. rubrum* was a dimer. We determined that the primary electron donor was the special pair.

In the Q_x band region, we observed a decrease in the MCD intensity; its magnitude was approximately 14% of the total by oxidation (Figure 1). Even if the residual part (35%) was taken into account, the expected value of the Q_x band was 19% of the total. The magnitude of the decrease in the RC preparation of *Rb. sphaeroides* (Figure 1, inset) was approximately 38%, and thus the decrease in *A. rubrum* was one-half. This difference indicates an optical feature that is essential for *A. rubrum*.

DISCUSSION

1. Molecular Organization of Cofactors in the RC Complex of A. rubrum. The optical properties of the RC complex of *A. rubrum* were essentially very similar to those of other purple bacterial RC in that the spectra consists of three bands (the primary electron donor, the accessory BChl, and BPheo), and the oxidized-minus-reduced difference spectra showed a bleach of the primary donor, a blue shift of the accessory BChl, and a red shift of BPheo (*18*, *19*). These indicate that the constitution and oxidation−reduction reaction of cofactors in *A. rubrum* RC were essentially similar to that in other purple bacteria.

Another significant optical feature of the RC preparation of *A. rubrum* was a clear signal from the Q_y^+ state; the ratio of intensity between the two states, Q_y^+/Q_y^- was approximately 0.3 in the deconvoluted absorption spectrum in the reduced state (Figure 3A). A higher exciton (Q_y^+) band has been demonstrated in the purple bacterial RC (*16*−*19*), although its intensity is usually low. The energy difference between the Q_y^+ and Q_y^- states, i.e., exciton splitting, was approximately 570 cm^{-1} for *A. rubrum* (Figure 3A) and approximately 900 cm^{-1} for *Rb. sphaeroides* (*16*−*19*). Since this energy difference is closely related to the strength of the interaction of the special pair, the organization of the dimer molecules in *A. rubrum* was expected to be different from that in purple bacteria. The other feature associated with the special pair was a decrease in the MCD intensity of the Q_x band (Figure 1C); its extent was nearly half that of *Rb. sphaeroides* (Figure 1C, inset). This indicates that only one-fifth of the pigments (Zn-BChl *a*) were bleached by oxidation. In the case of *Rb. sphaeroides*, the extent of the bleach reached about 38% of the total intensity, indicating that two BChl *a* molecules were bleached. By comparison with this result, it was suggested that a cation form of the special pair is localized in one pigment in the *A. rubrum* RC, which implies an essential difference in the molecular architecture of the special pair. Localization of the cation form on one Chl or BChl molecule has been reported for PS II RC (*32*) and purple bacterial RC (*33*−*36*). This interpretation is consistent with a smaller energy gap and a stronger signal from the upper exciton band than those found in other purple bacteria. According to the exciton theory (*37*), there is a high probability of transition to the upper exciton band caused by a tilted orientation between the components. This will result in a weaker interaction than that observed in a parallel orientation of two BChl *a* molecules.

The primary sequences of the L and M subunits of the *A. rubrum* RC complexes have already been reported (*38*). One important substitution was at position 168 in the L subunit; in *A. rubrum*, it is glutamic acid, while in other purple bacteria it is histidine. In *Rb. sphaeroides*, the His L 168 is hydrogen-bonded to the C_2 acetyl carbonyl group of BChl a_L of the special pair and determines the electrochemical potential of the special pair (*29*, *39*). Thus, in the case of *A. rubrum*, this replacement may influence the electronic properties of the special pair.

Table 1: Analysis of Component Bands by the Gaussian Deconvolution of the Spectra in the RC Preparation of *A. rubrum*[a]

absorption spectrum				CD spectrum			MCD spectrum				
location (nm)	ϵ (mM^{-1} cm^{-1})	width (cm^{-1})	D ($Debye^2$)	location (nm)	$\Delta\epsilon$ (M^{-1} cm^{-1})	width (cm^{-1})	location (nm)	$\Delta\epsilon_M$ (M^{-1} cm^{-1} T^{-1})	width (cm^{-1})	B ($Debye^2$) $k\beta/cm^{-1}$	B/D $k\beta/cm^{-1}$
					Reduced Form						
713.8	29.24	380					713.7	2.375	380		
749.9	120.5	845	74.64	737.5	−93.04	463	749.9	26.70	850	1782	23.9 (H)
792.0	238.5	409	75.52	791.1	580.1	325	791.8	56.23	408	1900	25.2 (B)
805.8	18.94	378		800.6	−791.5	204	805.7	18.05	378		
816.3	51.70	569									
844.6	68.83	790	44.89	841.5	198.0	905	844.5	7.606	790	531.3	11.8 (Q_y^-)
862.4	14.71	500	6.203	871.5	−3.170	310	862.3	1.564	498	70.26	11.3 (LH)
908.3	9.331	650									
					Oxidized Form						
713.8	32.13	380					713.7	2.658	380		
751.0	122.9	845	76.26	739.1	−92.09	470	750.9	26.50	845	1761	23.1 (H)
790.8	238.2	406	74.69	791.7	608.4	315	790.7	55.72	405	1868	25.0 (B)
805.8	6.058	375		801.3	−302.1	206	805.8	5.772	378		
816.4	51.70	569									
844.2	26.00	788	16.89	842.1	59.26	900	844.1	2.765	790	193.1	11.4 (Q_y^-)
862.4	14.71	500	6.203	871.5	−3.170	310	862.3	1.564	498	70.26	11.3 (LH)
908.3	10.72	650									

[a] D, B, and D/B are the dipole strength, the MCD intensity of the Faraday B-term, and their ratio, respectively. Width stands for full widths at half-maximum in wavenumber. H, B, P^-, and LH stand for BPheo *a*, accessory Zn-BChl *a*, the P^- state of the special pair, and LH 1, respectively.

There is still some ambiguity concerning the RC preparations since, in some cases, the residual part of the bleach by oxidation accounted for more than 70% of the total, even if there was no appreciable contamination of LH on SDS−PAGE. We interpret this as reflecting an inactivation of the RC during the preparation procedure. We found that the difference spectra induced by the oxidation reaction were similar to each other and only the magnitudes changed (data not shown). Thus, it is reasonable to conclude that the optical properties of the active RC are common to all preparations, as was shown in the present study. The inactive RC might have resulted from the treatment of the membranes and solubilized proteins with a higher pH (pH 8.8) than that used for growth (pH 3), to avoid the formation of aggregates.

2. Evolutionary Aspect in the Modified RC Complex in A. rubrum. Under the low-pH condition, Zn is highly soluble, allowing free Zn ions to be incorporated into BPheo *a*. However, Zn-BChl *a* must have two critical properties for the primary processes in photosynthesis: an electrochemical potential and a fluorescence yield, which are essential for the primary electron donor and antenna pigments, respectively. Replacement with Zn is only one means of keeping the above properties similar to those of Mg-BChl *a* (*5*). Clearly, a comparison of the reaction processes between Zn-BChl *a* and Mg-BChl *a* is critical for a fuller understanding of reaction mechanisms.

Since the radius of the Zn atom is larger than that of the Mg atom, the replacement of Mg with Zn is inevitably accompanied by protrusion of the central metal from the surface of the macrocycle. The dimer structure in the RC complex was formed by changing one amino acid residue from His L168 to Glu. However, the dimer structure was modified to a tilted orientation, according to our findings, which reflects a versatility in the primary process of bacterial photosynthesis. Replacement of one amino acid residue can cause spatial expansion of the dimer structure but may not be sufficient to hold the dimer in face-to-face stacking. Distribution of the cation might also be induced by the replacement. Even in the modified structure, the function of the BChl *a* dimer is completely preserved by Zn-BChl *a*, such that replacement of the central atom does not result in a malfunction of the modified RC. Our findings suggest that experiments on the RC complex with a replaced central metal can provide valuable information regarding the mechanism of the primary electron transfer in the bacterial RC and energy transfer in the antenna system. Since we do not yet know how the central metal is replaced during the synthetic pathways of BChl *a*, which is a main factor of the replacement in the acidic growth condition (*40*), future studies will attempt to elucidate that process.

REFERENCES

1. Wakao, N., Yokoi, N., Isoyama, N., Hiraishi, A., Shimada, K., Kobayashi, M., Kise, H., Iwaki, M., Itoh, S., Takaichi, S., and Sakurai, Y. (1996) *Plant Cell Physiol. 37*, 889−893.
2. Akiyama, M., Kobayashi, M., Kise, H., Takaichi, S., Watanabe, T., Shimada, K., Iwaki, M., Itoh, S., Ishida, N., Koizumi, M., Kano, H., Wakao, N., and Hiraishi, A. (1998) in *Photosynthesis: Mechanism and Effects* (Garab, G., Ed.) pp 731−734, Kluwer Academic Publishers, Dordrecht, The Netherlands.
3. Takaichi, T., Wakao, N., Hiraishi, H., Itoh, S., and Shimada, K. (1999) *Photosynth. Res. 59*, 255−256.
4. Shimada, K., Itoh, S., Iwaki, M., Nagashima, K. V. P., Matsuura, K., Kobayashi, M., and Wakao, N. (1998) in *Photosynthesis: Mechanism and Effects* (Garab, G., Ed.), pp 909−912, Kluwer Academic Publishers, Dordrecht, The Netherlands.
5. Kobayashi, M., Akiyama, M., Yamamura, M., Kise, H., Ishida, N., Koizumi, M., Kano, H., and Watanabe, T. (1998) in *Photosynthesis: Mechanism and Effects* (Garab, G., Ed.) pp 735−738, Kluwer Academic Publishers, Dordrecht, The Netherlands.
6. Kishimoto, N., Fukaya, F., Inagaki, K., Sugio, T., Tanaka, H., and Tano, T. (1995) *FEMS Microbiol. Ecol. 16*, 291−296.
7. Shimada, K. (1995) in *Anoxygenic Photosynthetic Bacteria* (Blankenship, R. E, Madigan, M. T., and Bauer, C. E., Eds.) pp 105−122, Kluwer Academic Publishers, Dordrecht, The Netherlands.
8. Dooley, D. M., and Dawson, A. J. (1994) *Coord. Chem. Rev. 60*, 1−15.

9. Kobayashi, M., Wang, Z.-Y., Yoza, K., Umetsu, M., Konami, H., Mimuro, M., and Nozawa, T. (1996) *Spectrochim. Acta 51A*, 585−598.
10. Nozawa, T., Mimuro, M., Kobayashi, M., and Tanaka, H. (1990) *Chem. Lett.* 2125−2128.
11. Nozawa, T., Kobayashi, M., Wang, Z.-Y., Itoh, S., Iwaki, M., Mimuro, M., and Satoh, K. (1995) *Spectrochim. Acta 51A*, 125−134.
12. Mimuro, M., Tomo, T., Nishimura, Y., Yamazaki, I., and Satoh, K. (1995) *Biochim. Biophys. Acta 1232*, 81−88.
13. Matsuura, K., and Shimada, K. (1986) *Biochim. Biophys. Acta 852*, 9−18
14. Ogata, T., Kodama, M., Nomura, S., Kobayashi, M., Nozawa, T., Katoh, T., and Mimuro, M. (1994) *FEBS Lett. 356*, 367−371.
15. Hoff, A. J., and Amesz, J. (1991) in *Chlorophylls* (Scheer, H., Ed.) pp 103−114, CRC Press, Boca Raton, FL.
16. Feher, G., and Okamura, M. Y. (1978) in *Photosynthetic Bacteria* (Clayton, R. K., Ed.) pp 349−386, Plenum Press, New York.
17. Parson, W. W. (1991) in *Chlorophylls* (Scheer, H., Ed.) pp 1153−1180, CRC Press, Boca Raton, FL.
18. Sauer, K., Dratz, E. A., and Coyne, L. (1968) *Proc. Natl. Acad. Sci. U.S.A. 61*, 17−24.
19. Sauer, K., and Lustin, L. A. (1978) *Biochemistry 17*, 2011−2019.
20. Houssier, C., and Sauer, K. (1970) *J. Am. Chem. Soc. 92*, 779−791.
21. Zevenhuijzen, D., and Zandstra, P. J. (1984) *Biophys. Chem. 19*, 121−129.
22. Sutherland, J. C., and Olson, J. M. (1981) *Photochem. Photobiol. 33*, 379−384.
23. Nozawa, T., Katano, T., Kudoh, M., Kobayashi, M., Shikama, Y., and Madigan, M. T. (1994) *Chem. Lett*. 193−196.
24. Philipson, K. D., and Sauer, K. (1973) *Biochemistry 12*, 535−539.
25. Nozawa, T., Trost, J. T., Fukada, T., Hatano, M., McManus, J. D., and Blankenship, R. E. (1987) *Biochim. Biophys. Acta 894*, 468−476.
26. Breton, J., Bylina, E. J., and Youvan, D. C. (1989) *Biochemistry 28*, 6423−6430.
27. Mar, T., and Gingras, G. (1995) *Biochemistry 34*, 9071−9078.
28. Deisenhofer, J., Epp, O., Miki, K., Huber, R., and Michel, H. (1985) *Nature 318*, 618−624.
29. Allen, J. P., Feher, G., Yeates, T. O., Komiya, H., and Rees, D. C. (1987) *Proc. Natl. Acad. Sci. U.S.A. 84*, 6162−6166.
30. Davis, C. M., Parkes-Loach, P. S., Cook, C. K., Meadows, K. A., Bandila, M., Scheer, H., and Loach, P. A. (1996) *Biochemistry 35*, 3072−3084.
31. Hartwich, G., Fiedor, L., Simonin, I., Cmiel, E., Schafer, W., Noy, D., Scherz, A., and Scheer, H. (1998) *J. Am. Chem. Soc. 120*, 3675−3683.
32. Noguchi, T., Inoue, Y., and Satoh, K. (1993) *Biochemistry 32*, 7186−7195.
33. Lendzian, F., Endeward, B., Plato, M., Bumann, D., Lubitz, W., Mobius, K., (1990) in *Reaction Centers of Photosynthetic Bacteria* (Michel-Beyerle, M. E., Ed.) pp 57−68, Springer-Verlag, Berlin.
34. Mattioli, T. A., Hoffmann, A., Robert, B., Schrader, B., and Lutz, M. (1991) *Biochemistry 30*, 4648−4654.
35. Plato, M., LeLendzian, F., Lubitz, W., Trankle, E., and Mobius, K. (1988) in *The Photosynthetic Bacterial Reaction Center, Structure and Dynamics* (Breton, J., and Vermeglio, D., Eds.) pp 379−388, Plenum Press, New York.
36. Plato, M., Mobius, K., Lubitz, W., Allen, J. P., and Feher, G. (1990) in *Perspective in Photosynthesis* (Jortner, J., and Pullman, B., Eds.) pp 423−434, Kluwer, Academic Publishers, Dordrecht, The Netherlands.
37. Kasha, M. (1963) *Radiat. Res. 20*, 55−71.
38. Nagashima, K. V. P., Matsuura, K., Wakao, N., Hiraishi, A., and Shimada, K. (1997) *Plant Cell Physiol. 38*, 1249−1258.
39. Lin, X., Murchison, H. A., Nagarajan, V., Parson, W. W., Allen, J. P., and Williams, J. C. (1994) *Proc. Natl. Acad. Sci. U.S.A. 91*, 10265−10269.
40. Masuda, T., Inoue, K., Masuda, M., Nagayama, M., Tamaki, A., Ohta, H., Shimada, H., and Takamiya, K. (1999) *J. Biol. Chem. 274*, 33594−33600.

BI991444E